ONLINE FIRST

ISSN: 0015-5659

e-ISSN: 1644-3284

Quantitative study of the popliteal fossa in the human fetus

Authors: Mateusz Badura, Maria Dąbrowska, Anna Badura, Monika Paruszewska-Achtel, Magdalena Grzonkowska, Mariusz Baumgart, Michał Szpinda

DOI: 10.5603/fm.98232

Article type: Original article

Submitted: 2023-11-16

Accepted: 2023-12-28

Published online: 2024-01-22

Quantitative study of the popliteal fossa in the human fetus

Mateusz Badura et al., Popliteal fossa measurements

Mateusz Badura[1], Maria Dąbrowska[1], Anna Badura[2], Monika Paruszewska-Achtel[1], Magdalena Grzonkowska[1], Mariusz Baumgart[1], Michał Szpinda[1, 3]

[1]Department of Normal Anatomy, Collegium Medicum in Bydgoszcz, Nicolaus Copernicus University in Torun, Bydgoszcz, Poland
[2]Department of Biopharmacy, Ludwik Rydygier Collegium Medicum in Bydgoszcz, Nicolaus Copernicus University in Torun, Bydgoszcz, Poland
[3]Medical Faculty, Academy of Applied Medical and Social Sciences, Elblag, Poland

Address for correspondence: Mateusz Badura, Department of Normal Anatomy, Collegium Medicum in Bydgoszcz, Nicolaus Copernicus University in Toruń, ul. Łukasiewicza 1, 85–821 Bydgoszcz, Poland, e-mail: m.badura@cm.umk.pl

ABSTRACT

The popliteal fossa presents an extensive diamond-shaped topographical element on the posterior aspect of the knee. With the use of classical anatomical dissection, digital image analysis of NIS Elements AR 3.0 and statistics we morphometrically analyzed the size of the popliteal fossa in human fetuses aged 17–29 weeks of gestation. Morphometric parameters of the popliteal fossa increased logarithmically with fetal age: $y = –44.421 + 24.301 \times \ln (Age)$ for length of superomedial boundary, $y = –41.379 + 22.777 \times \ln (Age)$ for length of superolateral boundary, $y = –39.019 + 20.981 \times \ln (Age)$ for inferomedial boundary, $y = –37.547 + 20.319 \times \ln (Age)$, for length of inferolateral boundary, $y = –28.915 + 15.822 \times \ln (Age)$ for transverse diameter, $y = –69.790 + 38.73 \times \ln (Age)$ for vertical diameter and $y = –485.631 + 240.844 \times \ln (Age)$ for projection surface area. Out of the four angles of the popliteal fossa the medial one was greatest, the inferior one the smallest, while the lateral one was somewhat smaller than the medial one and approximately three times greater than the superior one, with no difference with fetal age. In terms of morphometric parameters the popliteal fossa in the human fetus displays neither male-female nor right-left differences. In

the popliteal fossa, growth patterns of its four boundaries, vertical and transverse diameters, and projection surface area all follow natural logarithmic functions. All the morphometric data is considered age-specific reference intervals, which may be conducive in the diagnostics of congenital abnormalities in the human fetus.
Keywords: popliteal fossa, gastrocnemius muscle, semitendinosus muscle, semimembranosus muscle, plantaris muscle, biceps femoris muscle, human fetus

INTRODUCTION

The popliteal fossa presents an extensive topographical element on the posterior aspect of the knee, included between flexor muscles of thigh and flexor muscles of leg. The external contour of the popliteal fossa is diamond-shaped and covered with the popliteal fascia, which constitutes the roof of popliteal fossa [1, 2]. The popliteal fossa is bounded superomedially by the semitendinosus and semimembranosus muscles, superolaterally — by the biceps femoris muscle, inferomedially — by the medial head of gastrocnemius muscle, and inferolaterally — by the lateral head of gastrocnemius muscle and plantaris muscle [2–5]. All the aforementioned muscles flex and stabilize the knee joint [4, 6]. Apart from this, the semitendinosus muscle, semimembranosus muscle and lateral head of gastrocnemius muscle all medially rotate the leg (endororation), while the biceps femoris muscle and medial head of gastrocnemius are responsible for its lateral rotation (exorotation) [2, 4].

It should be emphasized that the floor of popliteal fossa is considerably greater than its roof. This is because the floor of popliteal fossa extends as high as the adductor hiatus and as low as the tendinous arch of soleus muscle [2, 4]. The floor of popliteal fossa is composed of the popliteal surface of femur, the articular capsule of knee joint with its oblique popliteal ligament and the popliteus muscle. According to Benniger and Delamarter [7], the oblique popliteal ligament is just the very first constituent of the trifurcation of the semimembranosus tendon, and so should be renamed to the oblique popliteal tendon or expansion. The second expansion of this trifurcation ends on the anteroinferior aspect of the medial condyle of tibia, the medial meniscus and the medial collateral ligament of knee, while the third one inserts onto the posteroinferior aspect of the medial condyle of tibia and provides fibers to the individual fascia of the popliteus muscle.

The popliteal fossa communicates anteriorly through the adductor hiatus with the adductor canal. Superiorly, the popliteal fossa is freely continuous with the flexor

compartment of thigh. Of note, the soleus muscle resembles a kind of diaphragm by separating the popliteal fossa from the deep part of flexor compartment of leg. Distally, the popliteal fossa communicates anteriorly with the extensor compartment of leg due to the opening above the interosseous membrane of leg that transmits the anterior tibial artery and veins. Deep to the tendinous arch of soleus muscle both the tibial nerve and posterior tibial vessels leave the popliteal fossa end enter the deep part of flexor compartment of leg [2, 4, 7]. The posterolateral corner of the knee is largely stabilized by the biceps femoris muscle, the head of fibula, the tendon of popliteus muscle, and the popliteofibular ligament [2, 8]. Of note, there is also the plantaris muscle, which is a small vestigial muscle with its incidence of 80–93% [9–11].

The popliteal fossa is traversed vertically by the popliteal artery and vein, both encompassed by the popliteal sheath. At the superior angle of popliteal fossa the sciatic nerve externally divides into the tibial and common fibular nerves. Not being included in the popliteal sheath, the tibial nerve freely winds from lateral to medial on the posterior aspect of popliteal vessels. The common fibular nerve traverses from the superior to lateral angle of popliteal fossa, and after leaving the popliteal fossa with level of the neck of fibula it divides into the superficial and deep fibular nerves [2, 12]. The popliteal fossa accommodates the popliteal lymph nodes, of which the middle popliteal lymph nodes clothe the popliteal vessels, the articular popliteal lymph node is between the oblique popliteal ligament and the popliteal artery, while the saphenous popliteal lymph node adheres to the junction of the small saphenous vein with the popliteal vein [2, 4, 9, 10].

The muscles limiting the popliteal fossa may indicate relevant variations, characterized by anomalous muscle slips that cross neurovascular structures and cause entrapment syndromes. The third head of gastrocnemius joining its medial head is most frequently quoted as producing such clinical problems [1, 3]. On the other hand, Liu et al. [6] presented the coexistence of bilateral absence of both the semimembranosus and quadratus femoris muscles.

After reviewing the professional literature we failed to find any morphometrical data concerning the popliteal fossa in the human fetus. Thus, we decided to morphometrically analyze the size of the popliteal fossa in human fetuses aged 17 to 29 weeks of gestation with the use of objective methods: digital image analysis and statistics. The present study provides new detailed numerical data of the popliteal fossa, so as to thoroughly understand its growth dynamics.

With relation to the popliteal fossa we aimed to examine:

— the possible variability of the muscles limiting the popliteal fossa that may considerably influence its morphometrical parameters;

— its size by performing its linear and planar measurements in order to achieve age-specific reference intervals of examined parameters;

— the possible right-left and male-female differences in all examined parameters; and

— growth patterns for all examined parameters.

MATERIALS AND METHODS

The examined material comprised 31 fetuses of both sexes, 17 males and 14 females, at the age of 17 to 29 weeks of gestation, derived from spontaneous miscarriages and preterm deliveries. The fetal collection of our Department of Normal Anatomy. The present examinations were ethically approved by the Bioethics Committee of the Ludwik Rydygier Collegium Medicum in Bydgoszcz, the Nicolaus Copernicus University in Bydgoszcz. The fetal ages were determined on the base of the crown-rump length. Table 1 presents characteristics of the examined fetal sample with its distribution to age, number and sex.

With the use of classical anatomical dissection on the posterior aspect of the lower limb the popliteal fossa was bilaterally exposed. The photographic documentation of the popliteal fossae was prepared by Canon EOS 70D(W), while in the morphometric analysis the system of digital image analysis NIS Elements AR 3.0 was involved. For each popliteal fossa its following 11 parameters were defined and measured (Fig. 1A–C):

— length of superomedial boundary (mm), extended between the superior and medial angles of popliteal fossa along the semitendinosus muscle;

— length of superolateral boundary (mm), extended between the superior and lateral angles of popliteal fossa along the biceps femoris muscle;

— length of inferomedial boundary (mm), extended between the inferior and medial angles of popliteal fossa along the medial head of gastrocnemius muscle;

— length of inferolateral boundary (mm), extended between inferior and lateral angles of popliteal fossa along the lateral head of gastrocnemius muscle;

— transverse diameter (mm), extended between the medial and lateral angles of popliteal fossa;

— vertical diameter (mm), extended between the superior and inferior angles of popliteal fossa;

— projection surface area (mm^2), calculated semiautomatically after the popliteal fossa was outlined;
— superior angle (α) of popliteal fossa, between the semitendinosus and biceps femoris muscles;
— medial angle (β) of popliteal fossa, between the semitendinosus muscle and medial head of gastrocnemius muscle;
— inferior angle (γ) of popliteal fossa, between the medial and lateral heads of gastrocnemius muscle; and
— lateral angle (δ) of popliteal fossa, between the lateral head of gastrocnemius muscle and biceps femoris muscle.

All numerical data was subject to statistical analysis with the use of STATISTICA 13.0. Because of the normal distribution of numerical data our results have been presented as means and standard deviations (SD). In order to compare right-left means and male-female means the t-Student test for dependent variables and the t-Student test for independent variables were respectively used with one-way analysis of variance. The growth patterns of particular morphometrical parameters were examined using linear and nonlinear regression analyses. The growth dynamics of best fit was unequivocally characterized and selected by the greatest value of its coefficient of determination (R^2). Statistically significant differences were considered at $p < 0.05$.

RESULTS

In the study material we found no variability concerning the skeletal muscles limiting the popliteal fossa, namely the semitendinosus, semimembranosus, biceps femoris, plantaris and gastrocnemius muscles that all follow typically without extra muscle slips. As a result, the shape of each popliteal fossa was regular and diamond-shaped.

The statistical analysis did not show any statistically significant male-female differences for all the parameters studied ($p > 0.05$), thus allowing us to aggregate them, without regard to sex (Tables 2–6).

Length values of the four boundaries of the popliteal fossa presented the following decreasing sequence: the superomedial, superolateral, inferolateral and inferomedial ones.

The mean length of superomedial boundary of popliteal fossa (Table 3A) increased from 6.205 ± 0.219 mm at week17 to15.221 ± 0.382 mm at week 29 of gestation on the right,

and from 6.321 ± 0.099 to 14.935 ± 0.106 mm respectively, without right-left differences ($p>0.05$). In the analyzed period the mean length of superomedial boundary of popliteal fossa followed the natural logarithmic function $y = –44.421 + 24.301 \times \ln (Age)$ with $R^2 = 0.897$ (Fig. 2A).

At the ages of 17–29 weeks of gestation, the mean length of superolateral boundary of popliteal fossa (Table 3A) increased its value from 5.395 ± 0.064 to 13.145 ± 0.106 mm on the right, and from 5.54 ± 0.028 to 13.225 ± 0.219 mm on the left, without right-left differences ($p > 0.05$). The mean length of superolateral boundary of popliteal fossa modelled the natural logarithmic function $y = –41.379 + 22.777 \times \ln (Age)$ with $R^2 = 0.862$ (Fig. 2B).

Between weeks 17 and 29, the mean length of inferomedial boundary of popliteal fossa (Table 3B) grew from 4.723 ± 0.212 to 13.195 ± 0.360 mm on the right, and from 4.755 ± 0.007 to 13.320 ± 0.424 mm on the left, without right-left differences ($p > 0.05$). The mean length of inferomedial boundary of popliteal fossa computed the natural logarithmic function $y = –39.019 + 20.981 \times \ln (Age)$ with $R^2 = 0.911$ (Fig. 2C).

The mean length of inferolateral boundary of popliteal fossa (Table 3B) revealed an increase in values from 5.34 ± 0.028 mm at week 17 to 11.53 ± 0.184 mm at week 29 on the right, and correspondingly from 5.765 ± 0.262 to 11.64 ± 0.849 mm on the left, without right-left differences ($P>0.05$). The mean length of inferolateral boundary of popliteal fossa generated the natural logarithmic function $y = –37.547 + 20.319 \times \ln (Age)$ with $R^2 = 0.860$ (Fig. 2D).

The vertical diameter of popliteal fossa was approximately twice its transverse diameter. Between weeks 17 and 29 of gestation the mean transverse diameter of popliteal fossa (Table 4) grew from 4.532 ± 0.070 to 10.735 ± 0.190 mm on the right, and from 4.695 ± 0.035 to 10.891 ± 0.184 mm on the left, without right-left differences ($p > 0.05$). The mean transverse diameter of popliteal fossa followed the natural logarithmic function $y = –28.915 + 15.822 \times \ln (Age)$, with $R^2 = 0.780$ (Fig. 2F).

The mean vertical diameter of popliteal fossa (Table 4) increased from 10.665 ± 0.488 mm at week 17 to 23.035 ± 0.544 mm at week 29 on the right, and correspondingly from 10.765 ± 0.021 to 22.695 ± 0.502 mm on the left. In the analyzed period the mean vertical diameter of popliteal fossa displayed the natural logarithmic function $y = –69.790 + 38.73 \times \ln (Age)$, with $R^2 = 0.901$ (Fig. 2E).

At the age range of 17–29 weeks, the mean projection surface area of popliteal fossa (Table 5) grew from 28.381 ± 0.707 to 101.195 ± 0.220 mm^2 on the right, and from 29.485 ±

0.898 to 101.195 ± 0.220 mm^2 on the left. The mean projection surface area of popliteal fossa modelled the natural logarithmic function y = –485.631 + 240.844 × ln (Age), with $R^2 = 0.936$ (Fig. 2G).

The four angles of the popliteal fossa presented the following decreasing sequence: the medial, lateral, superior and inferior ones. Their values did not significantly change with fetal age ($p > 0.05$).

The mean superior (α) angle of popliteal fossa (Table 6) between weeks 17 and 29 ranged from 38.172 ± 0.707 to 39.405 ± 0.007° on the right, and from 42.075 ± 6.230 to 40.500 ± 0.692° on the left, without statistically significant differences on either side and between left and right sides. At the same time, the mean medial (β) angle of popliteal fossa (Table 6) ranged from 141.085 ± 12.099 to 137.665 ± 1.846° on the right, and from 134.665 ± 5.509 to 137.835 ± 3.019° on the left, without statistically significant differences on either side and between left and right sides. The mean inferior (γ) angle of popliteal fossa (Table 6) between weeks 17 and 29 changed from 24.855 ± 10.798 to 40.430 ± 0.450° on the right, and from 22.611 ± 2.447 to 40.470 ± 2.447°, without statistically significant differences on either side and between left and right sides. The mean lateral (δ) angle of popliteal fossa (Table 6) reached the values of 133.695 ± 8.535° at week 17 and 135.58 ± 1.896° at week 29 on the right, and respectively 136.412 ± 2.659° and 136.321 ± 1.527° on the left side, without statistically significant differences on either side and between left and right sides.

DISCUSSION

The present discussion was separated into the following five subdivisions: sex and laterality differences of the popliteal fossa and its limiting muscles, numerical data of the popliteal fossa in the growing human fetus, variability of the muscles limiting the popliteal fossa, morphometric studies of the muscles limiting the popliteal fossa in the human fetus and clinical aspects of the popliteal fossa.

Sex and laterality differences of the popliteal fossa and its limiting muscles

In the material under examination we found the size of the popliteal fossa to be independent of both the sex and laterality. Since we failed to find any morphometric study of the popliteal fossa in the professional literature, we could not develop a comprehensive discussion about the sex and laterality differences of the popliteal fossa. However, after reviewing the medical literature we found the muscles limiting the popliteal fossa to be

independent of sex and laterality. This referred to the plantaris muscle [9], the triceps surae muscle [13], the biceps femoris muscle [14], the semimembranosus muscle [15] and the semitendinosus muscle [16]. All the aforementioned muscles displayed a commensurate increase in length and width, expressed by linear growth patterns. Szpinda et al. [17] alone reported the only laterality differences with relation to the short head of biceps femoris muscle. Neither sex nor laterality statistically significant differences were found in other skeletal muscles of the human fetus: the triceps brachii muscle [18], the biceps brachii muscle [19] and the rectus abdominis muscle [14] that extended typically from its origin to its insertion.

Numerical data of the popliteal fossa in the growing human fetus

Morphometric studies of the popliteal fossa may be conducive from both cognitive and clinical aspects. Dudek et al. [14] claimed that growing anatomical structures should be described accurately enough for clinical and prognostic purposes with segmental-linear models or one-function models. Furthermore, the degree of adjustment of model parameters and measurement results are strongly influenced by the function form, and especially by the size of anatomical structures. However, there are no reports in the professional literature to do with the size of the popliteal fossa in human fetuses. To the best of our knowledge the present article is the very first one to focus on the quantitative analysis on the popliteal fossa in the human fetus. Due to neither male-female nor right-left statistically significant differences ($p > 0.05$) we decided both aggregate numerical data concerning particular morphometric parameters and model only one growth pattern of statistical significance for each parameter. From a geometrical point of view, the diamond-shaped popliteal fossa presents a quadrangular with four sides and two diagonals. Having compared lengths of four boundaries of the popliteal fossa, we found the superomedial one to be greatest, the inferomedial one to be smallest, and the superolateral one to be greater than the inferolateral one. In the material under examination all these diameters elongate with fetal age in accordance with natural logarithmic functions. Lengths of the superomedial, inferomedial, superolateral and inferolateral boundaries of the popliteal fossa modelled the following natural logarithmic functions: $y = –44.421 + 24.301 \times \ln (Age)$, $y = –39.019 + 20.981 \times \ln (Age)$, $y = –41.379 + 22.777 \times \ln (Age)$ and $y = –37.547 + 20.319 \times \ln (Age)$, respectively.

As it turned out, the vertical diameter of popliteal fossa was roughly twice its transverse diameter. In the study period, both vertical and transverse diameters of the popliteal

fossa displayed the natural logarithmic growths: y = –69.790 + 38.73 × ln (Age) and y = –28.915 + 15.822 × ln (Age), correspondingly. Furthermore, the projection surface area of popliteal fossa increased in accordance with the natural logarithmic function y = –485.631 + 240.844 × ln (Age).

Out of the four angles of the popliteal fossa the medial one was greatest, the inferior one the smallest, while the lateral one was somewhat smaller than the medial one and approximately three times greater than the superior one.

The mean superior (α) angle of popliteal fossa (Table 6) between weeks 17 and 29 ranged from 38.172 ± 0.707 to 39.405 ± 0.007° on the right, and from 42.075 ± 6.230 to 40.500 ± 0.692° on the left, without statistically significant differences on either side and between left and right sides. Since the statistical analysis showed their values not to significantly change with fetal age ($p > 0.05$), we could not consequently model their growth patterns.

Variability of the muscles limiting the popliteal fossa

In the material under examination we did not find any variability of the skeletal muscles limiting the popliteal fossa: the semitendinosus, semimembranosus, biceps femoris, plantaris and gastrocnemius muscles that all extended in a typical fashion. Okamoto et al. [20] found an anomalous muscle to originate from the medial head of gastrocnemius, passed transversely subjacent to the popliteal fascia, crossed posteriorly to the neurovascular structures of the popliteal fossa to finally end on the biceps femoris tendon. Such an atypical muscle must have been derived from the short head of biceps femoris muscle, as it was innervated by the common peroneal nerve. Kim et al. [21] presented a similar thin transverse muscle in the superficial region of the popliteal region that however originated from the biceps femoris tendon and inserted onto the medial head of gastrocnemius muscle. It was innervated by a motor branch originating from the lateral sural cutaneous nerve and supplied by the sural artery.

The third head of gastrocnemius muscle presents its most common variation [1, 3, 22–24], found in 1.7–5.5% of individuals [3]. The third head of gastrocnemius muscle usually originates from the lateral epicondyle of femur, the lateral aspect of the popliteal surface of femur and the articular capsule of knee joint. It may sporadically originate from the long head of biceps femoris muscle, the lateral lip of linea aspera, the crural fascia, and even from the semitendinosus belly [3, 22–24]. The third head of gastrocnemius muscle typically descends

vertically subjacent to the popliteal fascia as the medial partner of the plantaris muscle, and inserts onto the junction of the medial and lateral heads of gastrocnemius muscle [3]. It may both possess some separate origins and divide near its insertion to merge with the two heads of gastrocnemius muscle. The biceps femoris muscle may either lack its short head or possess an extra head, originating from the ischial tuberosity, lateral lip of linea aspera or the lateral epicondyle of femur. Sinav et al. [25] found atypical muscle slips that underlay the popliteal fascia and fascia lata, respectively. The first one arose from the inferior part of the long head of biceps femoris muscle and ended in the crural fascia, while the other started with the superior part of the long head of biceps femoris muscle and joined the semitendinosus muscle. Liu et al. [6] and Sussmann [26] reported the bilateral absence of the semimembranosus muscle. Chason et al. [27] observed the tensor fasciae suralis, the belly of which originated from the lateral aspect of the semitendinosus muscle and extended to the distal thigh. Its long tendon superficially crossed the superficial popliteal fossa, so as to merge with the most superficial part of the calcaneal tendon.

Morphometric studies of the muscles limiting the popliteal fossa in the human fetus

Dudek et al. [14] examined the growth dynamics of the biceps femoris muscle, which is the superolateral boundary of the popliteal fossa, in 67 human fetuses of both sexes with the crown-rump length of 130–237 mm. Szpinda et al. [17] examined the biceps femoris muscle in 30 human fetuses aged 17–30 weeks of gestation. The growth of its long head followed commensurately in both length and width, and modelled linear functions: $y = –25.27 + 3.61 \times Age$ ($R = 0.90$) and $y = –2.75 + 0.35 \times Age$ ($R = 0.77$), respectively. Of note, the growth of the short head of biceps femoris presented the statistically significant right-left differences. Its length modelled the linear functions: $y = –10.09 + 1.86 \times Age$ ($R = 0.79$) on the right and $y = –4.45 + 1.58 \times Age$ ($R = 0.77$) on the left. Correspondingly, its width followed the linear functions: $y = –0.80 + 0.12 \times Age$ ($R = 0.54$) on the right and $y = 0.73 + 0.04 \times Age$ ($R = 0.25$) on the left. The length of tendon of biceps femoris muscle increase proportionately: $y = –9.85 + 1.41 \times Age$ ($R = 0.90$). Kadir et al. [13] performed the morphometric study of the gastrocnemius muscle in terms of its length, width and thickness in 51 human fetuses of both sexes aged 15–40 weeks of gestation. The medial head of gastrocnemius proved to be longer, wider and thicker than the lateral one. During the study period the length of medial and lateral heads of gastrocnemius muscle increased from 28.01 to 80.89 mm and from 14.77 to 53.54 mm, respectively. Yıldız et al. [9] examined the length and width of the plantaris belly and

tendon in 24 human fetuses aged 17–40 weeks of gestation. The plantaris muscle was absent unilaterally in one male fetus and bilaterally in one female fetus, while the remaining plantaris muscles were typically structured with a relatively short belly and long tendon. When compared the plantaris belly in the second and third trimesters of gestation, its mean length increased from 7.48 to 17.58 mm, while its mean width increased from 2.96 to 5.82 mm. As far as the plantaris tendon is concerned in the second and third trimesters of gestation, its mean length increased from 36.30 to 65.39 mm, while its mean width increased from 0.43 to 0.95 mm.

Badura et al. [15] examined the growth dynamics of the semimembranosus muscle in the human fetus that presents the superomedial boundary of the popliteal fossa. Both the length and width of the semimembranosus tendon modelled linear functions: $y = 0.058 + 0.992 \times Age$ ($R = 0.99$; $p < 0.05$) and $y = 0.068 + 0.940 \times Age$ ($R = 0.98$; $p < 0.05$), respectively. Another study by Badura et al. [16] concentrated on the fetal growth of the semitendinosus muscle that followed proportionately, as follows: $y = 9.8971 + 1.7803 \times Age$ ($R = 0.9752$; $p < 0.05$) for length of the semitendinosus belly, $y = –0.5495 + 0.207 \times Age$ ($R = 0.8729$; $p < 0.05$) for width of the semitendinosus belly, $y = –8.1735 + 1.4421 \times Age$ ($R = 0.9401$; $p < 0.05$) for length of the semitendinosus tendon and $y = 0.0097 + 0.0442 \times Age$ ($R = 0.8833$; $p < 0.05$) for width of semitendinosus tendon.

Clinical aspects of the popliteal fossa

An thorough understanding of both the topography and contents of the popliteal fossa is critical in patients suffering from its injury and other pathology [1]. Injuries of the popliteal fossa are sporadic, constitute only 2% of all surgical interventions around the knee, and mostly affect the plantaris muscle. Such a condition is clinically termed “tennis player’s leg” or “tennis leg” [11]. The injury of the plantaris muscle occurs most frequently while running or jumping and is caused by an eccentric load placed across the ankle with the extended knee [9]. Because of its long tendon and course with the calcaneal tendon, the plantaris muscle is commonly used for reconstruction of other tendons and ligaments, and may contribute to Achilles tendinopathy [11]. Isolated or combined chronic injury of the posterolateral corner of popliteal fossa requires its reconstruction with reconstruction of any concomitant cruciate ligament injury [8]. Damage to the soleus muscle mostly results from running or springing and is characterized by a severe pain after breaks, including a night rest.

Supernumerary muscles positioned at the inferior part of popliteal fossa constituted a much more frequent reason for entrapment of the popliteal vessels than those at the superior part of popliteal fossa [11, 13, 22, 24, 27, 28]. The third head of gastrocnemius muscle traverses the inferior part of popliteal fossa and may seriously exert a compressive effect on the adjacent neurovascular structures, usually resulting in the popliteal vessel entrapment or compressive neuropathies, involving branches of the tibial and common fibular nerves [3, 24]. Partial resection of the third head of gastrocnemius muscle is usually sufficient to relieve entrapped symptoms [22]. Kotian et al. [10] found a sporadic variation of the plantaris muscle to stem from a common origin with the further formation of two muscle bellies that crossed and entrapped the neurovascular bundle in the popliteal fossa. Olewnik et al. [11] presented an anomalous plantaris muscle that originated from the knee joint capsule, crossed posterior to the tibial nerve and the popliteal vessels, and might potentially exert a compression on the tibial nerve. Entrapment syndromes are characterized by a leg pain, tenderness in the popliteal fossa and decreased pulsations of the posterior tibial and dorsalis pedis arteries.

Chason et al. [27] and Montet et al. [28] emphasized that the tensor fasciae suralis muscle presents a sporadic cause of a popliteal mass, which must be differentiated from other pathological masses. Anatomical variations of the muscles limiting the popliteal fossa may be valuable for the surgical approaches in popliteal vessels syndromes [1]. Monotonous microtrauma of the pes anserinus, comprising tendons of the semitendinosus, gracilis and sartorius muscles, may lead to chronic inflammation and later result in development of degenerative changes in this region [29].

At the popliteal region may be localized neoplasmatic changes. Weschenfelder et al. [30] presented a desmoid tumor at the right popliteal fossa of a 34-year women. This tumor surrounded the lateral head of gastrocnemius muscle, involved the common fibular nerve, infiltrated the head of fibula as far as the posterolateral aspect of the articular capsule of knee joint. Derzsi et al. [31] described a hemangioma of the left popliteal fossa in a 13-year-child, who had previously undergone surgery because of the congenital pes equinovarus.

CONCLUSIONS

In terms of morphometric parameters the popliteal fossa in the human fetus displays neither male-female nor right-left differences.

In the popliteal fossa, growth patterns of its four boundaries, vertical and transverse diameters, and projection surface area all follow natural logarithmic functions.

All the morphometric data is considered age-specific reference intervals, which may be conducive in the diagnostics of congenital abnormalities in the human fetus.

REFERENCES

1. Ikiz ZAA, Ucerler H, Ozgur Z. Anatomic variations of popliteal artery that may be a reason for entrapment. Surg Radiol Anat. 2009; 31(9): 695–700, doi: 10.1007/s00276-009-0508-9, indexed in Pubmed: 19418007.
2. Szpinda M. Anatomia prawidłowa człowieka. Tom 1. Wyd. 1. Wydawnictwo Medyczne Edra Urban & Partner, Wrocław 2022.
3. Dave MR, Yagain VK, Anadkat S. Unilateral third/accessory head of the gastrocnemius muscle: a case report. Int J Morphol. 2012; 30(3):1061–1064.
4. Standring S. Gray's Anatomy: the anatomical basis of clinical practice. 44th Edition. Elsevier, London: 2021.
5. Tubbs RS, Caycedo FJ, Oakes WJ, et al. Descriptive anatomy of the insertion of the biceps femoris muscle. Clin Anat 2006; 19(6): 517–521, doi: 10.1002/ca.20168, indexed in Pubmed: 16283645.
6. Liu H, Fletcher J, Garrison MK, et al. Bilateral absence of quadratus femoris and semimembranosus. Int J Anat Var. 2011; 4: 40–42.
7. Benninger B, Delamarter T. Distal semimembranosus muscle-tendon-unit review: morphology, accurate terminology, and clinical relevance. Folia Morphol. 2013; 72(1): 1–9, doi: 10.5603/fm.2013.0001, indexed in Pubmed: 23749704.
8. Covey DC. Injuries of the posterolateral corner of the knee. J Bone Joint Surg Am. 2001; 83: 106–118, doi: 10.2106/00004623-200101000-00015, indexed in Pubmed: 11205847.
9. Spina AA. The plantaris muscle: anatomy, injury, imaging, and treatment. J Can Chiropr Assoc. 2007, 51(3), 158 – 165, indexed in Pubmed: 17885678.
10. Kotian SR, Sachin KS, Bhat KMR. Bifurcated plantaris with rare relations to the neurovascular bundle in the popliteal fossa. Anat Sci Int. 2013; 88(4): 239–241, doi: 10.1007/s12565-013-0184-z, indexed in Pubmed: 23771697.
11. Olewnik Ł, Podgórski M, Polguj M, et al. The plantaris muscle – rare relations to the neurovascular bundle in the popliteal fossa. Folia Morphol. 2018, 77(4): 785–788, doi: 10.5603/FM.a2018.0039, indexed in Pubmed: 29651792

12. Chetty D, Pillay PL, Lazarus L, et al. The common fibular nerve (and its branches) in fetuses. Int J Morphol. 2014; 32(2): 455–460.

13. Kadir D, Ceren U, Busra S, et al. A study on the structure and morphologic development of calcaneal tendon and triceps surae muscle in human fetuses during the fetal period and the evaluation of clinical importance of calcaneal tendon. Int J Morphol. 2015; 33(3): 920–929.

14. Dudek K, Kędzia W, Kędzia E. et al. Mathematical modelling of the growth of human fetus anatomical structures. Anat Sci Int. 2017; 92(4): 521 – 529, doi: 10.1007/s12565-016-0353-y, indexed in Pubmed: 27393150.

15. Badura M, Wiśniewski M, Szpinda M, et al. Developmental dynamics of the semimembranosus muscle in human foetuses. Med Biol Sci. 2011; 25: 13–16.

16. Badura M, Wiśniewski M, Szpinda M, et al. The growth of the semitendinosus muscle in human foetuses. Med Biol Sci. 2011; 25: 17–21.

17. Szpinda M, Wiśniewski M, Rolka Ł. The biceps femoris muscle in human fetuses – a morphometric, digital and statistical study. Adv Clin Exp Med. 2011; 20(5): 575–582.

18. Grzonkowska M, Badura M, Lisiecki J, et al. Growth dynamics of the triceps brachii muscle in the human fetus. Adv Clin Exp Med. 2014; 23(2): 177–184, doi: 10.17219/acem/37045, indexed in Pubmed: 24913107.

19. Szpinda M, Paruszewska-Achtel M, Baumgart M, et al. The normal growth of the biceps brachii muscle in human fetuses. Adv Clin Exp Med. 2013; 22(1): 17–26, indexed in Pubmed: 23468258.

20. Okamoto K, Wakebe T, Saiki K, et al. An anomalous muscle in the superficial region of the popliteal fossa, with special reference to its innervation and derivation. Ann Anat. 2004; 186(5–6): 555–559, doi: 10.1016/S0940-9602(04)80106-7, indexed in Pubmed: 15646291.

21. Kim DI, Kim HJ, Shin C, et al. An abnormal muscle in the superficial region of the popliteal fossa. Anat Sci Int. 2009; 84(1–2): 61–63, doi: 10.1007/s12565-008-0002-1, indexed in Pubmed: 19214656.

22. Iwai T, Sato S, Yamada T, et al. Popliteal vein entrapment caused by the third head of the gastrocnemius muscle. Br J Surg. 1987; 74(11): 1006–1008, doi: 10.1002/bjs.1800741117, indexed in Pubmed: 3690223.

23. Bergman RA. Compendium of human anatomic variation: text, atlas and world literature. Urban & Schwarzenberg, Baltimore 1988.

24. Bergman RA, Walker CW, El-Khour GY. The third head of gastrocnemius in CT images. Ann Anat 1995 177(3): 291–294, doi: 10.1016/s0940-9602(11)80205-0, indexed in Pubmed: 7598226

25. Sinav A, Gümüşalan Y, Arifoğlu Y, et al. Accessory muscular bundles arising, from biceps femoris muscle. Kaibogaku Zasshi. 1995; 70(3): 245–247, indexed in Pubmed: 7645372.

26. Sussmann AR. Congenital bilateral absence of the semimembranosus muscles. Skeletal Radiol. 2019; 48(10): 1651–1655, doi: 10.1007/s00256-019-03210-3, indexed in Pubmed: 30982941.

27. Chason DP, Schultz SM, Fleckenstein JL. Tensor fasciae suralis: depiction on MR images. Am J Roentgenol. 1995; 165(5): 1220–1221, doi: 10.2214/ajr.165.5.7572507, indexed in Pubmed: 7572507.

28. Montet X, Sandoz A, Mauget D, et al. Sonographic and MRI appearance of tensor fasciae suralis muscle, an uncommon cause of popliteal swelling. Skeletal Radiol 2002; 31(9): 536–538, doi: 10.1007/s00256-002-0496-x, indexed in Pubmed: 12195508.

29. Rowicki K, Płomiński J. Bachta A. Evaluation of the effectiveness of platelet rich plasma in treatment of chronic pes anserinus pain syndrome. Ortop Traumatol Rehabil. 2014; 16(3): 307–318, doi: 10.5604/15093492.1112532, indexed in Pubmed: 25058106.

30. Weschenfelder W, Lindner R, Spiegel C, et al. Desmoid Tumor of the Popliteal Fossa during Pregnancy. Case Rep Surg. 2015, doi: 10.1155/2015/262654, indexed in Pubmed: 25734019.

31. Derzsi Z, Gurzu S, Jung I, et al. Arteriovenous synovial hemangioma of the popliteal fossa diagnosed in an adolescent with history of unilateral congenital clubfoot: case report and a single-institution retrospective review. Rom J Morphol Embryol. 2015; 56 (2), 2: 549–552, indexed in Pubmed: 26193227.

Table 1. Characteristics of the examined fetal sample with its distribution to age, number and sex

Gestational Age	Crown-rump length (mm)		Number of fetuses	Sex	
Weeks	Mean	SD		♂	♀
17	117.5	0.707	2	2	
18	136.5	7.778	2	1	1
19	151	2.517	3	2	1
20	167	1.414	2	1	1
21	176	3.512	3	2	1
22	182.5	0.707	2		2
23	195	4.243	2		2
24	211.5	0.707	2	1	1
25	216.5	2.121	2	1	1
26	231	2.828	2	1	1
27	241.4	2.121	2	1	1
28	247.5	1.708	4	1	3
29	260.5	0.707	3	1	2
Total			31	14	17

Table 2. Regression analysis for examined parameters of the popliteal fossa with age

Parameter	Regression formulae related to age	R^2	F	P
Superomedial border [mm]	y = –44.421 + 24.301 × ln (Age)	0.897	535.1	=0.00
Superolateral border [mm]	y = –41.379 + 22.777 × ln (Age)	0.862	377.2	= 0.00
Inferomedial border [mm]	y = –39.019 + 20.981 × ln (Age)	0.911	614.5	= 0.00
Inferolateral border [mm]	y = –37.547 + 20.319 × ln (Age)	0.860	369.6	= 0.00
Length [mm]	y = –69.790 + 38.730 × ln (Age)	0.901	548.7	= 0.00
Width [mm]	y = –28.915 + 15.822 × ln (Age)	0.780	213.3	= 0.00
Surface area [mm^2]	y = –485.631 + 240.844 × ln (Age)	0.936	879.0	= 0.00

Table 3A. Statistical analysis of numerical data of the length of superomedial and superolateral boundary (mean ± SD) of the popliteal fossa

Gestational age [weeks]	Number of fetuses	Length of superomedial boundary				Length of superolateral boundary			
		Right		Left		Right		Left	
		Mean	SD	Mean	SD	Mean	SD	Mean	SD
17	2	6.205	0.219	6.320	0.099	5.395	0.064	5.540	0.028
18	2	6.875	0.191	6.945	0.021	6.040	1.457	6.045	1.407
19	3	9.230	1.127	9.550	1.190	8.820	1.134	9.110	1.169
20	2	9.745	0.926	9.765	0.841	10.495	0.530	9.995	0.078
21	3	10.270	0.242	10.980	0.554	10.27	0.806	10.650	0.860
		(P<0.01)				(P<0.01)			
22	2	10.115	0.106	10.540	0.099	10.575	0.488	10.175	0.219
23	2	11.525	0.658	12.000	0.226	10.350	0.523	10.925	0.954
24	2	11.410	0.778	10.680	0.481	10.445	0.290	10.885	0.035
25	2	10.635	0.573	10.945	0.672	10.715	0.530	10.175	0.205
26	2	11.870	0.014	11.500	0.608	12.785	0.346	12.290	0.438
		(P<0.01)				(P<0.01)			
27	2	13.035	0.643	13.380	0.848	12.845	0.346	13.085	0.021
28	4	14.570	0.360	14.715	0.184	13.765	0.396	13.320	0.454
29	3	15.220	0.382	14.935	0.106	13.145	0.106	13.225	0.219
		(P<0.01)				(P<0.01)			

Table 3B. Statistical analysis of numerical data of the length of inferomedial and inferolateral boundary (mean ± SD) of the popliteal fossa

Gestational age [weeks]	Number of fetuses	Length of inferomedial boundary				Length of inferolateral boundary			
		Right		Left		Right		Left	
		Mean	SD	Mean	SD	Mean	SD	Mean	SD
17	2	4.720	0.212	4.755	0.007	5.340	0.028	5.765	0.262
18	2	5.940	0.127	5.900	0.042	6.340	1.061	5.955	0.559
19	3	6.910	0.590	6.450	0.757	6.070	0.569	6.470	0.974
20	2	7.410	0.976	7.320	1.541	7.720	1.626	7.365	2.213
21	3	8.810	0.378	8.790	0.796	8.180	0.700	9.020	0.523
		(P<0.01)				(P<0.01)			
22	2	7.845	0.247	7.995	0.785	7.125	0.559	7.060	0.325
23	2	8.740	0.580	9.030	0.424	8.655	0.672	9.185	0.855
24	2	8.800	1.131	8.880	1.188	8.220	0.594	8.465	0.728
25	2	9.545	0.516	9.575	0.318	9.630	0.283	9.860	0.184
26	2	10.215	0.389	10.155	0.530	10.035	0.629	10.110	0.877
		(P<0.01)				(P<0.01)			
27	2	10.735	0.290	10.685	0.474	11.695	0.049	11.305	0.389
28	4	11.245	0.258	11.390	0.352	11.365	1.306	11.470	0.906
29	3	13.195	0.361	13.320	0.424	11.530	0.184	11.640	0.085
		(P<0.01)				(P<0.01)			

Gestational age [weeks]	Number of fetuses	Vertical diameter [mm]				Transverse diameter [mm]			
		Right		Left		Right		Left	
		Mean	SD	Mean	SD	Mean	SD	Mean	SD
17	2	10.665	0.488	10.765	0.021	4.530	0.071	4.695	0.035
18	2	11.745	0.389	11.605	0.304	5.155	0.205	5.190	0.297
19	3	14.420	0.734	14.130	0.784	5.030	0.358	5.060	0.325
20	2	17.245	1.492	16.455	1.195	5.020	0.679	4.835	0.318
21	3	17.290	1.124	18.160	1.200	7.050	1.603	6.810	0.111
		(P<0.01)				(P<0.01)			
22	2	17.350	0.891	17.140	0.749	6.260	0.509	6.130	0.551
23	2	19.600	0.085	20.130	0.523	6.790	0.042	6.600	0.382
24	2	19.015	0.276	18.680	0.594	7.635	1.534	7.560	2.164
25	2	21.495	1.421	20.845	0.671	8.510	0.099	8.865	0.035
26	2	22.515	3.472	22.050	1.457	8.460	0.198	8.475	0.403
		(P<0.01)				(P<0.01)			
27	2	21.335	1.860	20.975	1.619	9.680	0.113	9.460	0.622
28	4	24.055	0.044	24.075	0.561	8.400	0.290	8.235	0.191
29	3	23.035	0.544	22.695	0.502	10.735	0.191	10.890	0.184
		(P<0.01)				(P<0.01)			

Table 4. Statistical analysis of numerical data of the vertical and transverse diameters (mean ± SD) of the popliteal fossa

Table 5. Statistical analysis of numerical data of the projection surface area (mean ± SD) of the popliteal fossa

Gestational age (weeks)	Number of fetuses	Projection surface area [mm^2]			
		Right		Left	
		Mean	SD	Mean	SD
17	2	28.380	0.707	29.485	0.898
18	2	34.620	1.669	34.485	1.761
19	3	38.550	0.959	38.030	0.836
20	2	38.760	0.382	38.185	0.092
21	3	45.720 (P<0.01)	0.692	44.160	1.317
22	2	49.225	0.785	48.380	0.848
23	2	63.535	5.537	62.370	5.614
24	2	73.110	6.307	70.055	2.779
25	2	70.855	0.969	72.290	2.744
26	2	78.910 (P<0.01)	0.042	80.065	2.595
27	2	92.895	16.440	91.605	13.781
28	4	101.055	3.107	99.720	3.661
29	3	101.600 (P<0.01)	1.527	101.195	0.219

Table 6. Statistical analysis of numerical data of the four angles (mean ± SD) of the popliteal fossa

Gestational age [weeks]	Number of fetuses	Superior (α) angle				Medial (β) angle				Inferior (γ) angle				Lateral (δ) angle			
		Right		Left		Right		Left		Right		Left		Right		Left	
		Mean	SD	Mean	SD	Mean	SD	Mean	SD	Mean	SD	Mean	SD	Mean	SD	Mean	SD
17	2	38.17	0.707	42.075	6.230	134.66	5.508	141.08	12.098	34.85	10.797	22.60	2.446	133.69	8.534	136.4	2.659
18	2	36.53	7.001	36.655	7.163	134.30	7.530	130.33	6.484	34.08	10.472	44.77	1.704	126.28	3.649	133.72	0.035
19	3	39.65	4.643	39.65	5.282	129.04	1.0515	129.66	0.647	44.72	5.284	45.98	0.911	136.57	2.232	136.48	2.391
20	2	35.19	4.101	36.045	1.167	141.96	2.121	137.90	3.443	40.18	1.485	39.30	0.735	137.74	6.117	138.31	8.429
21	3	37.99	2.598	36.22	2.782	139.35	6.736	138.44	9.031	39.82	3.165	39.74	3.621	141.76	5.488	141.88	4.631
		(P<0.01)				(P<0.01)				(P<0.01)				(P<0.01)			
22	2	35.25	5.565	36.30	3.989	142.53	3.811	141.93	3.234	45.67	2.170	47.28	5.374	132.64	4.264	135.98	0.480
23	2	37.29	5.728	40.535	2.552	141.85	7.170	140.71	8.019	40.23	2.984	40.45	1.414	146.55	4.229	138.54	4.080
24	2	37.06	6.993	35.20	5.756	134.47	9.291	135.43	9.376	43.28	3.854	43.81	1.627	133.96	8.026	134.75	7.658
25	2	32.95	2.270	31.665	1.902	144.17	2.340	145.85	0.035	38.30	0.460	38.80	1.167	141.77	5.105	141.98	4.808
		(P<0.01)				(P<0.01)				(P<0.01)				(P<0.01)			
26	2	37.11	2.998	39.13	7.085	144.36	0.990	144.81	2.107	33.11	8.959	31.86	10.628	136.52	10.394	132.39	1.407
27	2	40.46	1.506	39.22	0.297	144.14	5.883	144.09	6.123	39.08	0.424	38.80	0.841	132.82	2.008	134.02	1.725
28	4	36.06	3.573	37.96	3.474	137.91	4.658	141.91	1.719	38.84	3.462	37.29	4.768	145.30	4.305	141.15	2.886
29	3	39.40	0.007	40.50	0.693	137.83	3.019	137.66	1.846	40.43	0.4957	40.47	0.778	135.58	1.895	136.32	1.527
		(P<0.01)				(P<0.01)				(P<0.01)				(P<0.01)			

Figure 1. The popliteal fossa in a female fetus at 22 weeks showing the measured parameters (**A–C**); 1 — length of superomedial boundary; 2 — length of superolateral boundary; 3 — length of inferomedial boundary; 4 — length of inferolateral boundary; 5 — vertical diameter; 6 — transverse diameter; 7 — projection surface area; superior (α) angle, medial (β) angle, inferior (γ) angle and lateral (δ) angle of popliteal fossa.

Figure 2. Regression lines for the length of superomedial boundary (**A**), superolateral boundary (**B**), inferomedial boundary (**C**), inferolateral boundary (**D**), vertical diameter (**E**), transverse diameter (**F**) and projection surface area (**G**) of the popliteal fossa.

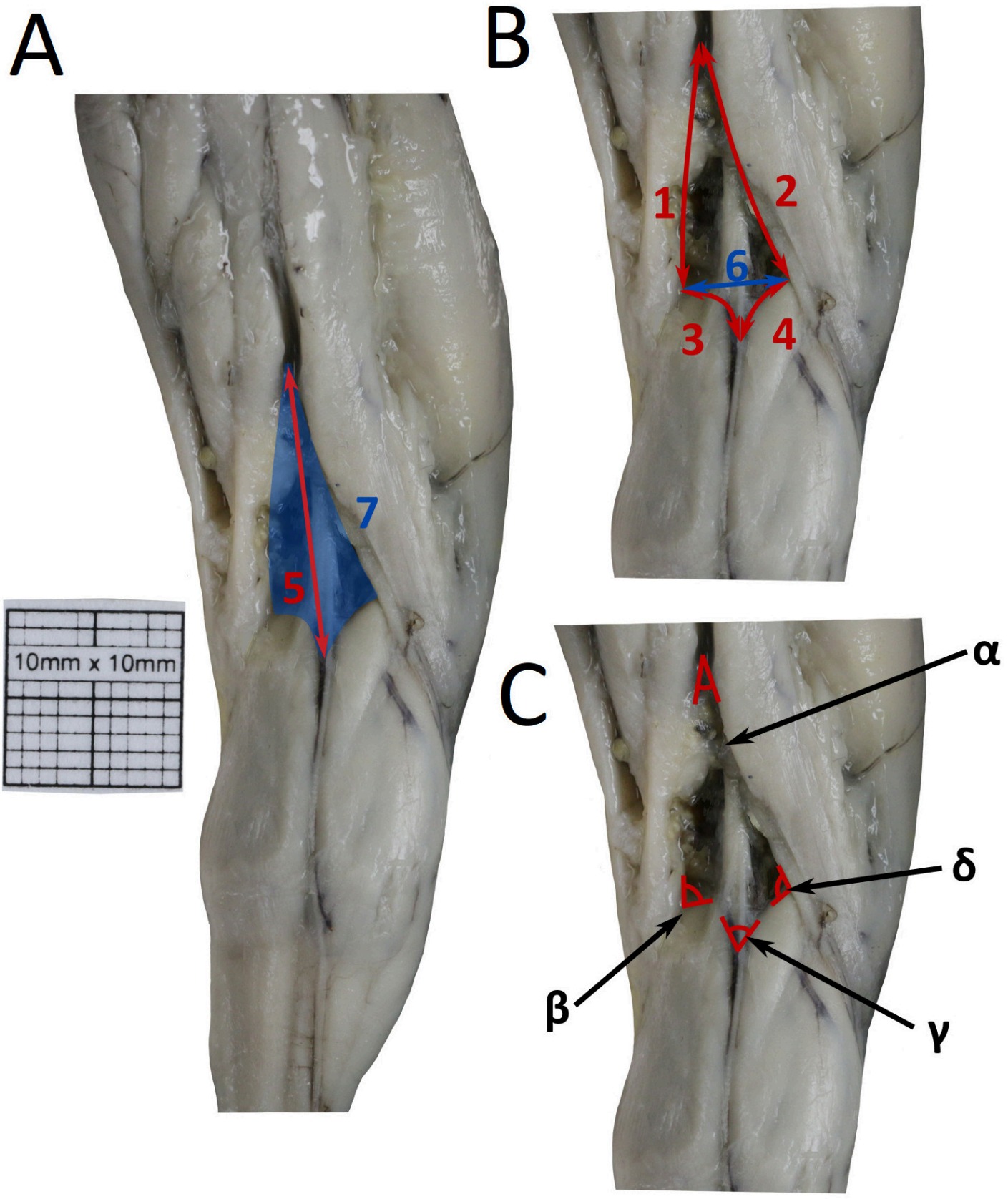
A
10mm x 10mm
5
7
B
1
2
3
4
6
C
A
α
β
γ
δ

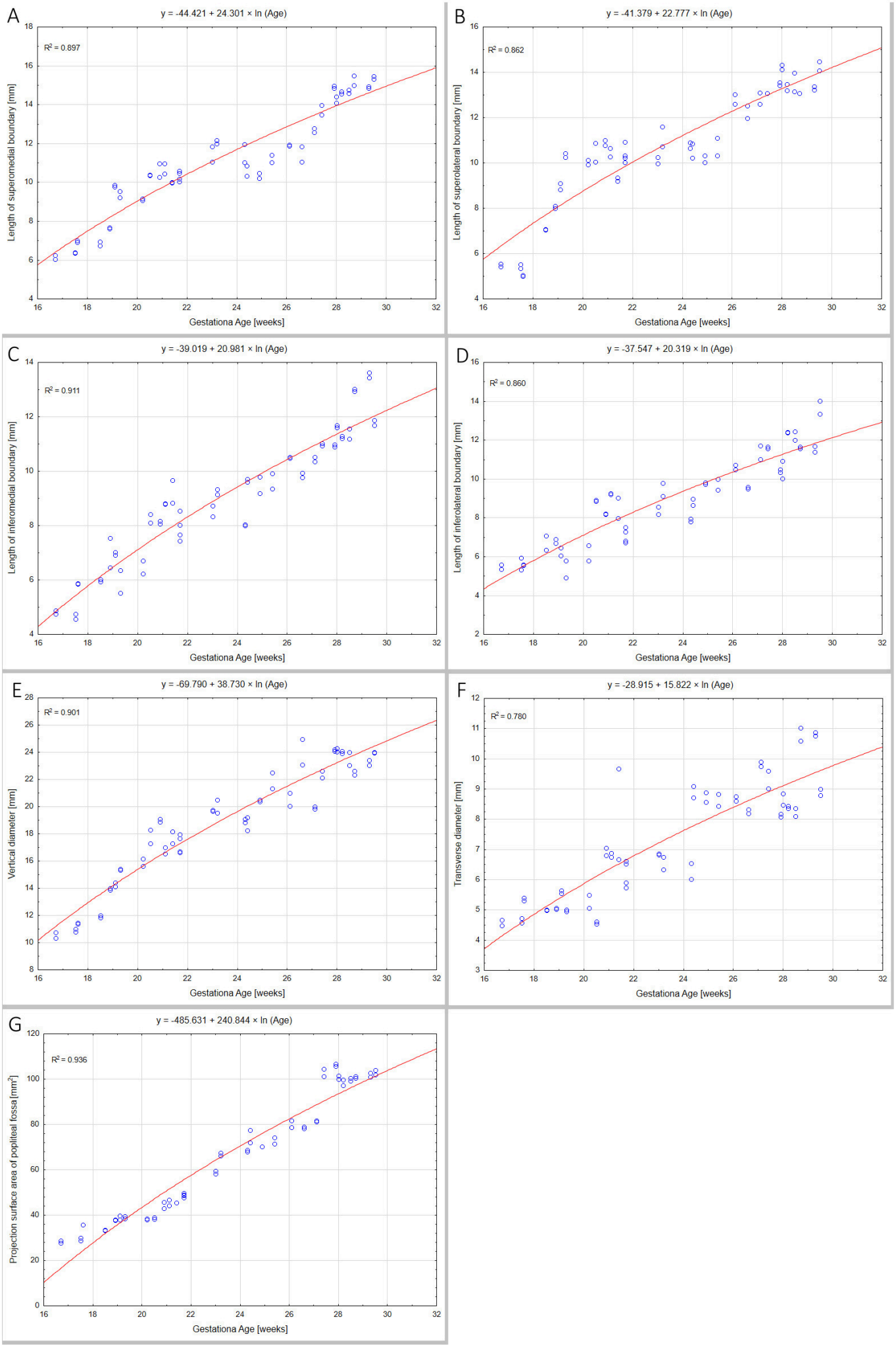
A
y = -44.421 + 24.301 × ln (Age)
R² = 0.897
Length of superomedial boundary [mm]
Gestationa Age [weeks]
B
y = -41.379 + 22.777 × ln (Age)
R² = 0.862
Length of superolateral boundary [mm]
Gestationa Age [weeks]
C
y = -39.019 + 20.981 × ln (Age)
R² = 0.911
Length of inferomedial boundary [mm]
Gestationa Age [weeks]
D
y = -37.547 + 20.319 × ln (Age)
R² = 0.860
Length of inferolateral boundary [mm]
Gestationa Age [weeks]
E
y = -69.790 + 38.730 × ln (Age)
R² = 0.901
Vertical diameter [mm]
Gestationa Age [weeks]
F
y = -28.915 + 15.822 × ln (Age)
R² = 0.780
Transverse diameter [mm]
Gestationa Age [weeks]
G
y = -485.631 + 240.844 × ln (Age)
R² = 0.936
Projection surface area of popliteal fossa [mm²]
Gestationa Age [weeks]